Supplementary Information

Using the Plasmon Linewidth to Calculate the Time and Efficiency of Electron Transfer between Gold Nanorods and Graphene

*Anneli Hoggard[1,2], Lin-Yung Wang[1,2], Lulu Ma[3], Ying Fang[1,2], Ge You[3], Jana Olson[1,2], Zheng Liu[3], Wei-Shun Chang[1,2], Pulickel M. Ajayan[3], Stephan Link[1 2,4]**

[1]Department of Chemistry, [2]Laboratory for Nanophotonics, [3]Department of Mechanical Engineering and Materials Science, and [4]Department of Electrical and Computer Engineering, Rice University, Houston, Texas 77005, United States

*Address correspondence to slink@rice.edu

Contents

1. Gold Nanorod Characterization

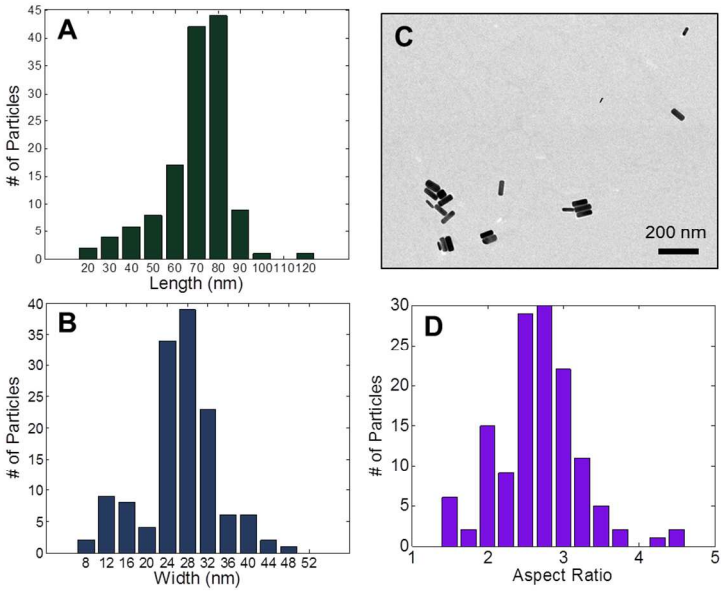

Figure S1. Histograms of gold nanorod length (A) and width (B) obtained from TEM. A representative TEM image is shown in (C). Nanorod aspect ratios (length/width) were also calculated (D).

The nanorod sample contained a distribution of sizes as indicated by the transmission electron microscopy (TEM) analysis shown in Figure S1. Average values were as follows: length = 70 ± 16 nm, width = 27 ± 7.4 nm, and aspect ratio = 2.7 ± 0.5. The nanorod size distribution gave rise to an inhomogeneously broadened extinction spectrum, as illustrated in Figure S2. The ensemble resonance energy and linewidth were 1.7 eV and 214 meV, respectively.

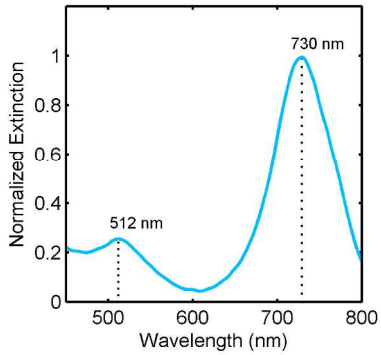

Figure S2. UV-vis extinction spectrum of the gold nanorod sample in solution. The longitudinal and transverse plasmon resonances are labeled at 730 nm and 512 nm, respectively.

2. Optical Microscopy and SEM Correlation

In order to verify the presence of individual gold nanorods instead of small aggregates, several nanorods measured optically were correlated with scanning electron microscopy (SEM). Figure S3 shows an SEM image (A) with a corresponding dark-field scattering image (B), illustrating that indeed isolated single nanorods were measured within the limited optical resolution. Similar nanorod densities were also observed for the graphene sample (Figure S4).

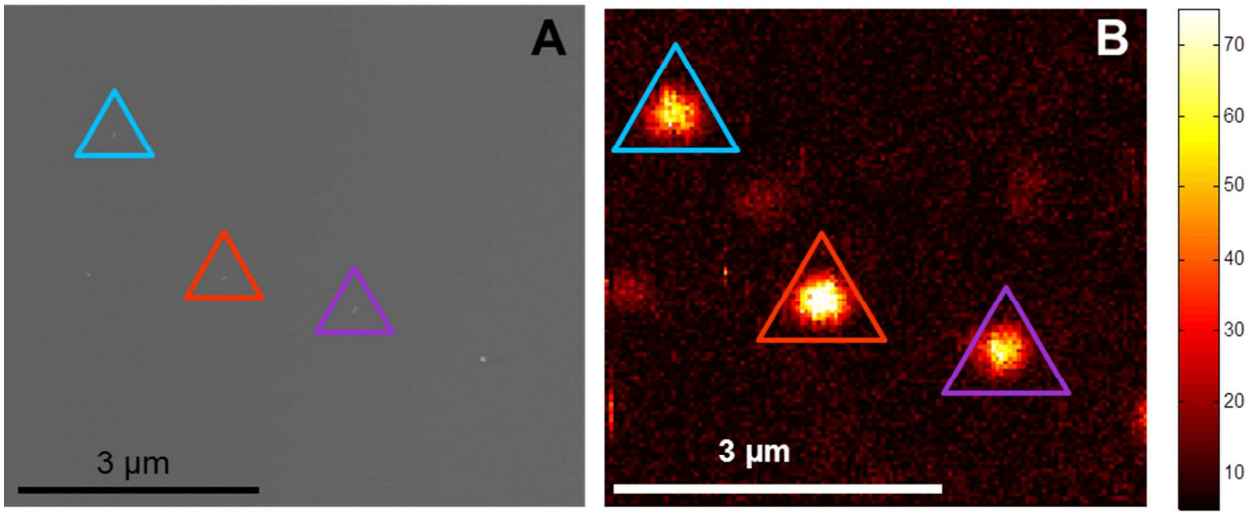

Figure S3. A SEM micrograph (A) of 3 single nanorods and their corresponding dark-field scattering intensity image (B).

3. Graphene Characterization

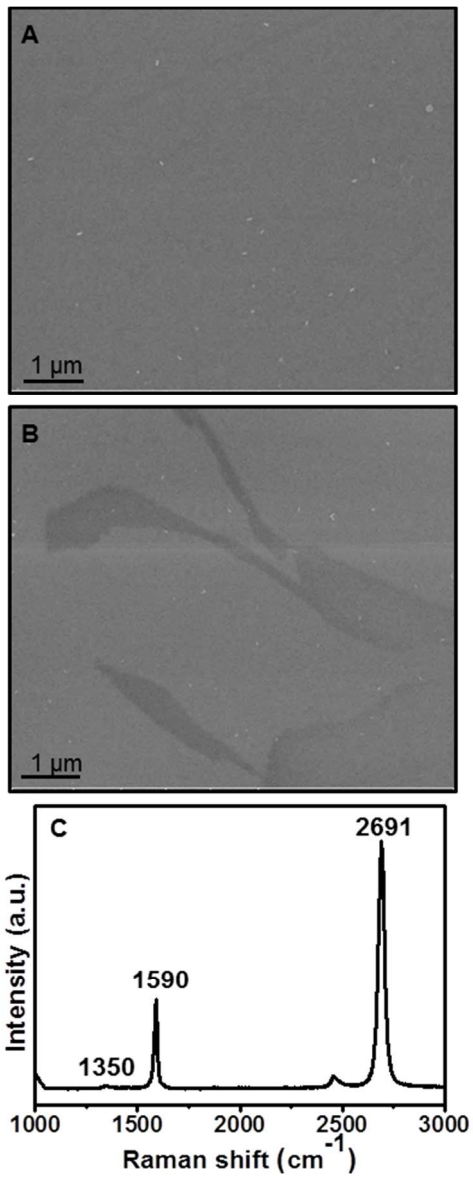

Figure S4. (A) SEM image of gold nanorods on graphene. The density of gold nanorods was comparable to the one on quartz slides (Figure S3). Some small holes in the graphene layer are visible as dark lines in the SEM image. (B) SEM image showing more pronounced holes in the graphene layer. Graphene is more conductive than the quartz slide, and therefore the exposed quartz areas appear comparatively darker in the SEM images. Large area holes in the graphene layer could also be observed in the optical microscope and were avoided in the single particle spectroscopy studies. (C) Typical Raman spectrum recorded with 514.5 nm laser excitation (Renishaw inVia) of the graphene sample used showing the characteristic lines expected for single-layer graphene. The disorder-induced Raman D peak at ~1350 cm^{-1} is very weak, indicating the high quality of the CVD-grown graphene. The G and 2D peaks are found at 1590 and 2691 cm^{-1}, respectively. The intensity ratio of G to 2D peak is ~3 for most areas of the sample, indicating the presence of single-layer graphene.[1]

4. Single Particle Spectroscopy Set-Up

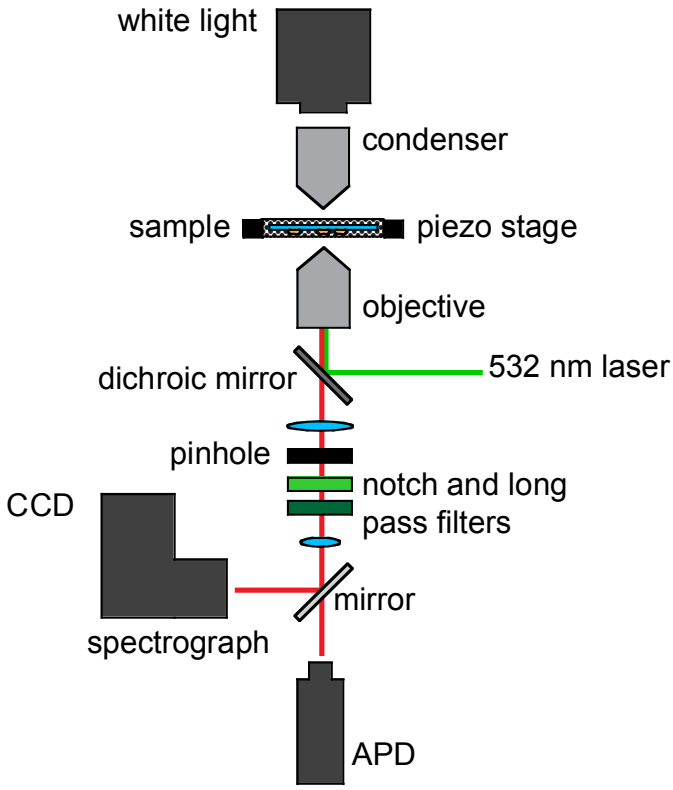

Figure S5. The optical set-up used for single particle dark-field scattering and photoluminescence measurements.

Figure S5 illustrates the experimental setup of the single particle spectrometer. For dark-field scattering measurements, the dichroic, notch, and long pass filters were removed. The pinhole was required to eliminate excess background scattering. For the photoluminescence measurements, the dichroic, notch, and long pass filters were necessary to completely remove the laser excitation light. The pinhole was not used for the photoluminescence measurements because the spatial extent of the signal was determined by the size of the laser focus, which we determined to be ~ 380 nm by calibration with fluorescent beads.

5. FDTD Calculations

Classical electrodynamics simulations of gold nanorods were carried out using a commercially available finite-difference-time-domain (FDTD) package.[2] The model geometry is shown in Figure S6. The energy-dependent optical constants of gold were adopted from the tabulated values for bulk gold measured by Johnson and Christy.[3] The quartz substrate was modeled as a SiO_2 dielectric layer with a refractive index of 1.65.[4-5] Because the chemically-prepared gold nanorods contained cetyl trimethylammonium bromide (CTAB) double layers on the surface, a 2-nm thick dielectric layer ($\varepsilon_{CTAB} = 4.0$) was also included in the model.[5] The width and length dispersions of the gold nanorods (exclusive of the CTAB layer) were accounted for by modeling nanorods with widths of 26 ± 4 nm and lengths of 70 ± 8 nm, which were varied in 2 nm increments. These values were chosen to reflect the experimental size distribution (Figure S1). The minimum grid size used in the simulations was 1 nm, and default convergence criteria were used. The calculations were carried out using the Shared Tightly-Integrated Cluster (STIC) provided by Rice University. Each job required 36 CPUs with approximately one hour run time. Examples of the calculated scattering spectra are shown in Figure S7.

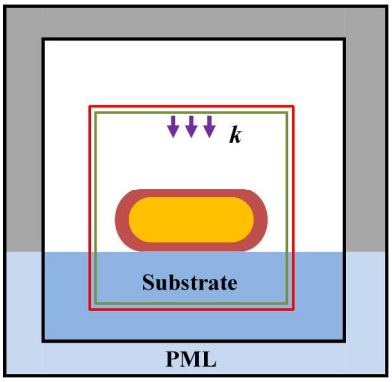

Figure S6. Schematic illustration of the geometry used in the FDTD calculations. The hemispherically-capped cylinder geometry was chosen to approximate the nanorod shape. The nanorods were surrounded by a 2-nm-thick dielectric layer (shown in red) to model the CTAB coating. The green box represents the total-field-scatter-field (TFSF) input light source. The wave vector *k* was perpendicular to the substrate and the electric field component was circularly polarized. The red box represents the discrete Fourier transform (DFT) monitors enclosing both the nanorods and the substrate. The perfect matching layer (PML) was split into two parts with the upper region matching the air environment and the lower part matching the dielectric substrate, which was modeled to extend into the PML.

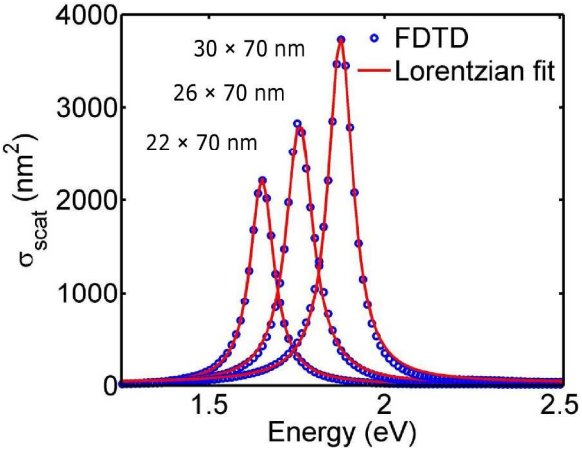

Figure S7. Calculated scattering spectra (blue data points) using the FDTD method. Lorentzian fits (red lines) yielded the linewidth and the energy of the longitudinal plasmon resonance.

6. Plasmon Linewidth Modeling

The theoretically expected plasmon linewidth was calculated using a quasi-static model following the procedure described by Sönnichsen *et al.* [6] The nanorod polarizability α along the longitudinal axis was calculated using the following equation[7]:

$$\alpha_i = \left(\frac{V_{clust}\varepsilon_0}{L_i}\right)\left(\frac{1-\varepsilon_r}{\left(\frac{1}{L_i}-1\right)+\varepsilon_r}\right) \quad \text{with} \quad L_i = \left(1+\frac{a}{b}\right)^{-1.6} \quad \text{and} \quad \varepsilon_r = \frac{\varepsilon(\omega)}{\varepsilon_m}$$

where $\varepsilon(\omega)$ is the bulk gold dielectric function that depends on the frequency ω, ε_m is the frequency-independent dielectric constant of the surrounding medium, V_{clust} is the nanorod volume, and a and b are the major and minor axes of an ellipsoid. The medium dielectric constant to approximate the experimental conditions was chosen to be 1.5. The scattering cross section was calculated using the following relationship[8]:

$$\sigma_{sca} = \frac{k^4}{6\pi}\left(\left|\frac{\alpha}{\varepsilon_0}\right|\right)^2 \text{ with } k = \frac{2n_m\pi}{\lambda}$$

where ε_0 is the permittivity of free space, λ is the wavelength, and n_m is the refractive index of the surrounding medium. Spectra were calculated using this model for different aspect ratios of gold nanorods, and from the Lorentzian fits to the spectra the dependence of linewidth on the plasmon resonance energy were obtained.

Because the above model describes the surface plasmon resonance for nanorods with sizes that fall within the quasi-static limit, the contribution of radiation damping to the total plasmon linewidth is not included. As the nanorods studied were large enough to require such contribution though, we included radiation damping via $\Gamma_{rad} = 2\hbar\kappa V$ where κ is the radiation damping coefficient and V is the nanorod volume. To account for the nanorod sample size dispersity, a linear approximation of nanorod volume as a function of resonance energy, $V(E)$, was used for the calculations in Figure 4. The linear approximation was derived as follows: First, the nanorod aspect ratio was converted to resonance energy using the calculated spectra. Next, nanorod volumes were calculated as a function of aspect ratio from the TEM data in Figure S1. Finally, with the conversion between aspect ratio and resonance energy, the dependence of the volume on the resonance energy was obtained and binned into intervals of 0.05 eV. Figure S8

shows this dependence of the volume on resonance energy. Aspect ratios ranging from 2.0 to 4.5 were required to describe the range of resonance energies observed experimentally.

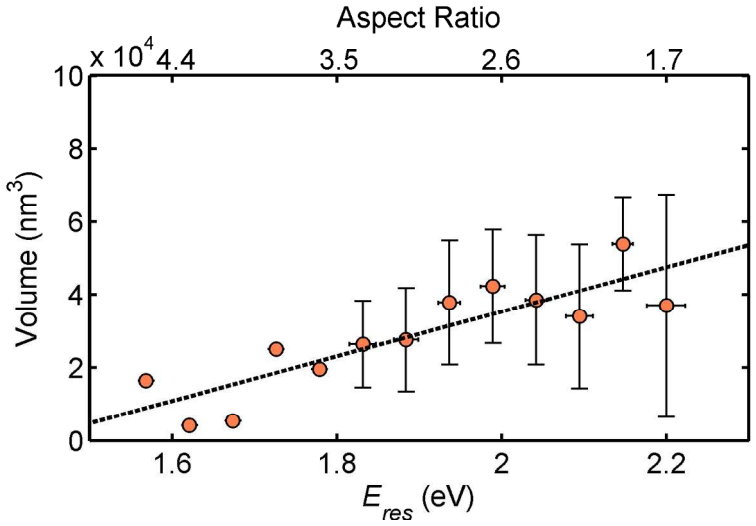

Figure S8. Nanorod volume vs. aspect ratio and resonance energy as determined by the quasi-static model and from the TEM data. The linear trend (line) was used to estimate the nanorod volume for the calculation of the radiation damping contribution to the plasmon linewidth. Data was binned into 0.05 eV increments, and error bars represent the standard deviation.

7. Additional Single Particle Spectroscopy Results

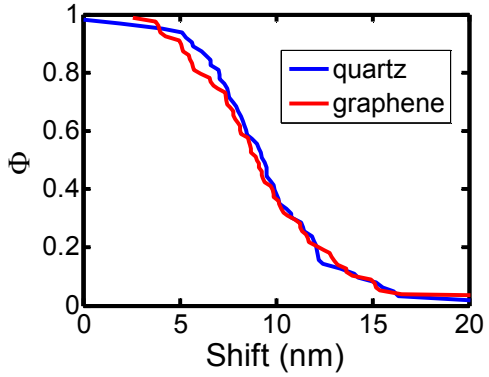

Figure S9. Complementary cumulative distributions of the wavelength shift between the plasmon resonance maxima measured in the photoluminescence and dark-field scattering spectra of single gold nanorods on quartz (blue) and graphene (red).

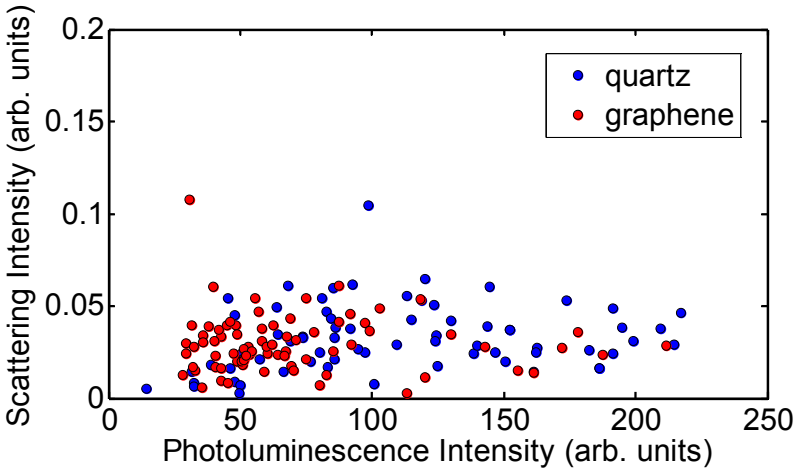

Figure S10. Photoluminescence intensity vs. dark-field scattering intensity for the longitudinal surface plasmon resonance plotted of single nanorods on quartz (blue) and graphene (red). For the intensity values, the peak intensity at the resonance maximum was chosen.

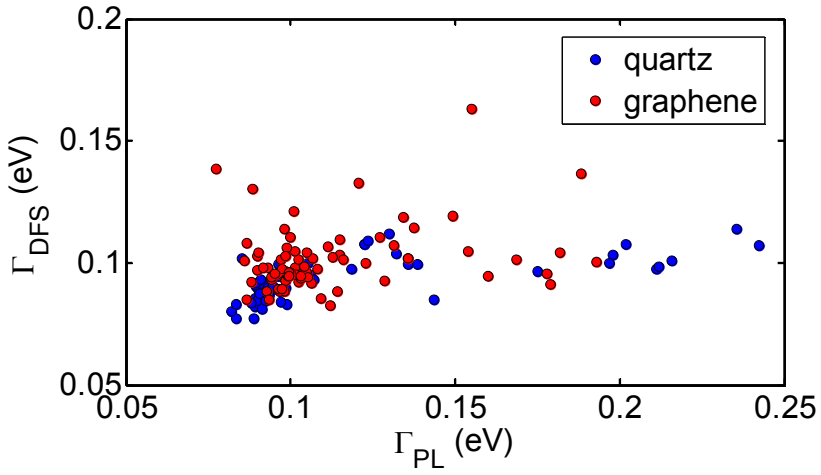

Figure S11. Photoluminescence linewidth vs. the scattering linewidth of the longitudinal surface plasmon resonance of single gold nanorods on quartz (blue) and graphene (red).

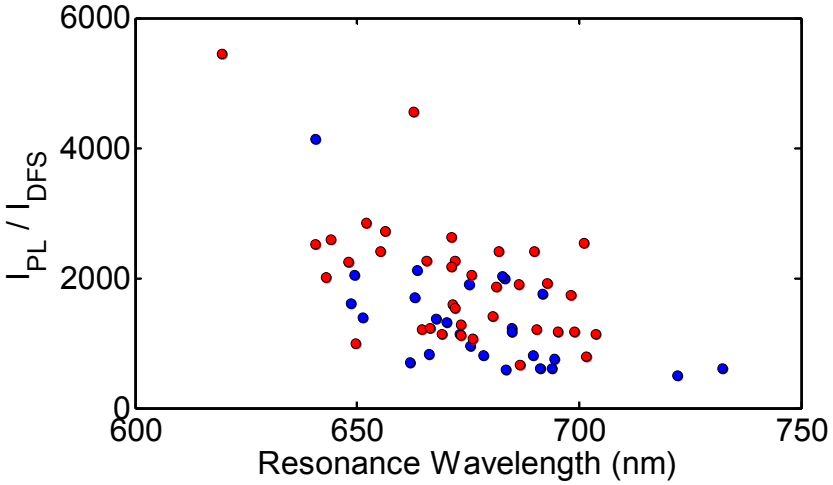

Figure S12. Photoluminescence (PL) intensity normalized by the dark-field scattering (DFS) intensity plotted vs. the maximum of the longitudinal surface plasmon resonance of single gold nanorods on quartz (blue) and graphene (red).

8. References

1. Ferrari, A. C.; Meyer, J. C.; Scardaci, V.; Casiraghi, C.; Lazzeri, M.; Mauri, F.; Piscanec, S.; Jiang, D.; Novoselov, K. S.; Roth, S.*, et al*, Raman Spectrum of Graphene and Graphene Layers. *Phys. Rev. Lett.* **2006,** *97*, 187401.
2. *FDTD Solutions* 8.5.3; Lumerical Solutions, Inc: Vancouver, Canada, 2013.
3. Johnson, P. B.; Christy, R. W., Optical Constants of the Noble Metals. *Phys. Rev. B* **1972,** *6*, 4370-4379.
4. Palik, P. D., *Handbook of Optical Constants of Solids* Academic Press: Orlando, 1985.
5. Slaughter, L. S.; Wu, Y.; Willingham, B. A.; Nordlander, P.; Link, S., Effects of Symmetry Breaking and Conductive Contact on the Plasmon Coupling in Gold Nanorod Dimers. *ACS Nano* **2010,** *4*, 4657-4666.
6. Sönnichsen, C.; Franzl, T.; Wilk, T.; von Plessen, G.; Feldmann, J.; Wilson, O.; Mulvaney, P., Drastic Reduction of Plasmon Damping in Gold Nanorods. *Phys. Rev. Lett.* **2002,** *88*, 077402.
7. Kreibig, U., Vollmer, M., *Optical Properties of Metal Clusters*. Springer: Berlin, 1995.
8. Novotny, L.; Hecht, B., *Principles of Nano-Optics*. Cambridge University Press: Cambridge, 2012.